A zircon U-Pb study of the evolution of lunar KREEP

By A.A. Nemchin, R.T. Pidgeon, M.J. Whitehouse, J.P. Vaughan and C. Meyer

Abstract

SIMS U-Pb analyses show that zircons from breccias from Apollo 14 and Apollo 17 have essentially identical age distributions in the range 4350 to 4200 Ma but, whereas Apollo 14 zircons additionally show ages from 4200 to 3900 Ma, the Apollo 17 samples have no zircons with ages <4200 Ma. The zircon results also show an uneven distribution with distinct peaks of magmatic activity. In explaining these observations we propose that periodic episodes of KREEP magmatism were generated from a primary reservoir of KREEP magma, which contracted over time towards the centre of Procellarum KREEP terrane.

Introduction

One of the most enigmatic features of the geology of the Moon is the presence of high concentrations of large ion lithophile elements in clasts from breccias from non mare regions. This material, referred to as KREEP *(1)* from its high levels of K, REE and P, also contains relatively high concentrations of other incompatible elements including Th, U and Zr. Fragments of rocks with KREEP trace element signatures have been identified in samples from all Apollo landing sites *(2)*. The presence of phosphate minerals, such as apatite and merrillite *(3)*; zirconium minerals, such as zircon *(4)*, zirconolite *(5)* and badelleyite *(6)*, and rare earth minerals such as yttrobetafite *(7)*, are direct expressions of the presence of KREEP. Dickinson and Hess *(8)* concluded that about 9000 ppm of Zr in basaltic melt is required to saturate it with zircon at about 1100^{o}C (the saturation concentration increases exponentially with

increasing temperature). They estimated that for KREEP basalt 15382 zircon saturation would occur after 88% crystallisation just before immiscibility is reached, whereas crystallsiation of Ti-basalt 70017, with an initial Zr concentration of 200 ppm, would have about 2000 ppm of Zr at the onset of immiscibility and an additional 80% crystallisation would be required to achieve zircon saturation. An important implication of their results is that only KREEP rich magma can produce zircon (i.e. that there is an intimate link between the original enrichment of a melt in a KREEP component and the appearance of zircon in the rock that crystallised from this melt). This association of zircon with KREEP in several rock types provides an opportunity to place time constraints on KREEP evolution throughout lunar history. One of the most important consequences of this association is that the oldest zircon provides a younger age limit for the generation of a late residual melt which concentrated incompatible elements, referred to as urKREEP by Warren and Wasson *(9)*, during cooling and differentiation of the lunar magma ocean (LMO).

Whereas in lunar rocks and minerals Rb/Sr, Sm/Nd ratios are generally unfavourable for precise age determinations, and these geochronological systems, together with K-Ar, are prone to disturbance by thermal events associated with impacts, zircon is well known for its stability under high temperature conditions *(10)*. The zircon U-Pb system also has the advantage that a number of precise SIMS analyses can be made on individual zircon grains to check the internal consistency of the ages, thus avoiding possible problems from analysing mineral separates or whole rock samples with more than one age. SIMS determined zircon U-Pb ages for lunar rocks have been reported by Compston et al. *(11)*, Meyer et al. *(4)* and Pidgeon et al. *(12)*. Meyer et al. *(13)* comment that zircons formed early in lunar history and have

survived many impacts and associated thermal events. Thus they give important information about the age of plutonic rocks from the original lunar crust.

The purpose of this contribution is to present new SIMS U-Pb analyses on lunar zircons from samples of breccias from the Apollo 14 and 17 landing sites. These data represent an overview of our total data set and include analyses of zircons located in individual clasts and those that occur as loose grains in the breccia matrix. We discuss the distribution of the ages and their implications for the early history of the Moon.

Zircon samples and SIMS U-Pb results

U and Pb isotopes were measured using SHRIMP II at Curtin University of Technology (Perth, Western Australia) and CAMECA IMS1270 ion microprobe at the Museum of Natural History in Stockholm (Sweden) *(14)*.

The present zircon samples are from a random collection of 16 thin sections from Apollo 14 and 17 breccias and a sawdust sample from Apollo 14 specimen 14321. The mode of occurrence of the zircons, either as components of breccia clasts (18 grains) or as separate xenocrysts in the breccia matrix (46 grains) is briefly indicated in Table 1. However, the mode of occurrence of the 15 zircons analysed from a sawdust sample from breccia 14321 is uncertain. 60 out of a total number of 79 analysed zircon grains are from the Apollo 14 landing site. The remaining 19 grains are from Apollo 17 samples. In the following discussion we assume that zircons from the sections and the sawdust sample are approximately representative of zircons in the rocks from the two sites. Apollo 14 breccias are generally interpreted to represent the Fra Mauro formation, which is considered to be primary Imbrium ejecta *(e.g. 15)*, although Haskin et al. *(16)* and Morrison and Oberbeck *(17)* argued that this

formation was derived from local material together with ejecta from the Imbrium impact. Impact melt breccias from the Apollo 17 mission have been interpreted as reflecting the formation of the Serenitatis basin *(e.g. 18)*. As most analyses are concordant within analytical uncertainty (Fig. 1) the distribution of $^{207}Pb/^{206}Pb$ ages is used in discussing the age profiles. When more than one analysis is reported for a grain (Table S1), the oldest $^{207}Pb/^{206}Pb$ age is considered to represent the primary age of this grain and is included in histograms and probability plots showing age distribution for Apollo 14 and Apollo 17 zircons presented in Figure 2.

Zircon age profiles

The most striking result of the present study is the comparison between the zircon age profiles from the Apollo 14 and Apollo 17 landing sites. Both Apollo 14 and Apollo 17 zircons have essentially identical age patterns in the age range 4350 – 4200 Ma but, whereas Apollo 14 zircons also have ages in the range 4200 to 3900 Ma, the Apollo 17 samples have no zircons with ages < 4200 Ma.

If real, the absence of zircons with ages younger than 4200 Ma in Apollo 17 samples has significant implications for KREEP evolution. However, the first question to be asked is whether this can be simply a consequence of the sample sizes, particularly given the smaller number of Apollo 17 zircon analyses. Sixteen out of sixty zircons from analysed Apollo 14 samples have ages younger than 4200 Ma, and if it is assumed that the proportion of <4200 Ma grains is the same in rocks from both sites at least five zircons of that age would be expected to occur in the 19 analysed grains from Apollo 17 rocks. The probability of overlooking these younger grains in Apollo 17 samples is a function of n, the number of zircon grains analysed and X, the proportion of younger grains in the total population. This probability is given by *(1-*

$X)^n = (1\text{-}16/60)^{19}$=0.0028 or about 0.3% *(19)*. If only grains younger than 4100 Ga are considered this probability increases to about 6.5%, which still leaves little doubt that the lack of grains younger than 4200 Ma in rocks from the Apollo 17 region is real and that the observed age distribution patterns suggest that a significant time difference exists in the lateral distribution of KREEP magmatic activity on the Moon.

Zircon age peaks

Meyer et al. *(4)* found that zircon U-Pb ages of lunar granophyres extended from 4.32 Ga to 3.88 Ga and suggested that the zircon forming lunar magmatism was most active prior to 4.30 Ga and continued until at least 3.88 Ga. However, results obtained from the present study show that this continuum of ages is not smooth but consists of a number of distinctive age peaks with surrounding troughs (Fig. 2). In the Apollo 14 zircon age distribution peaks of KREEP magmatism are recorded at ~4350 Ma, ~4200 Ma and possibly ~4000 Ma. Only a few ages are younger than 4000 Ma. In addition there are age troughs at ~ 4250 Ma and ~4100 Ma. The Apollo 17 distribution also shows peaks at 4350 Ma and 4200 Ma and a trough at 4250 Ma, but has no ages younger than 4200 Ma. Peaks at the above ages are present in lunar granophyric zircon ages of Meyer et al *(4)*. The zircon ages are generally interpreted as dating magmatic events *(e.g. 4)* and the interpretation of the zircon age peaks as marking periodic episodes of KREEP magmatism has profound implications for understanding lunar evolution. However, important concerns are whether the age peaks could be influenced by sample selection or whether, despite earlier views, they could reflect major resetting events of the zircon U-Pb systems.

It is possible the small data set could be biased by including analyses of a number of cogenetic zircons from a single igneous clast. However the majority of

zircons from breccia matrices have a range of ages and U and Th contents and appear to be independent grains. Only in a clast in section 14303-49 is it evident that the zircons are nearly the same age and are potentially cogenetic. However, it makes no significant difference to the age distribution if only one zircon U-Pb analysis, instead of the four analysed zircons from this clast, is included in the age distribution calculation.

Whereas it has been a long held assumption that the lunar zircon ages record magmatic crystallisation events it has been demonstrated *(12, 20)* that zircon grains from lunar samples can undergo partial, inhomogeneous, or even complete isotopic disturbance, induced by a marginally younger event (or events). Therefore the possibility must be considered that some zircon ages represent resetting events in response to massive impacts. All analyses presented in Table S1 are clustered near the concordia line, which makes it difficult to separate zircons with primary ages from grains that have experienced partial Pb-loss. However, the internal homogeneity of analysed zircon grains with respect to age, U and Th concentrations and internal structure provide a sound basis for distinguishing zircons with primary crystallisation ages from those with disturbed U-Pb systems.

Twenty seven zircon grains from the Apollo 14 samples and fifteen grains from the Apollo 17 samples were large enough to accommodate two or more analyses (Table S1). Only seven of these grains, including the complex grain 73235-82 described by Pidgeon et al. *(20)*, show significant variation of their $^{207}Pb/^{206}Pb$ ages ages. Multiple analyses of most grains with reproducible $^{207}Pb/^{206}Pb$ ages are also homogeneous in U and Th concentration. Our conclusion is that the analysed zircons are dominantly magmatic undisturbed grains. A few grains included in the distribution

have experienced some isotopic disturbance. For these grains the oldest age is taken as representing the primary age of the grain.

The formation of breccias at both landing sites have been attributed to impact events at ~ 3900 Ma (Imbrium impact at ~3850 Ma, *(21)* for the Apollo 14 breccias and Serenitatis impact at 3893± 9 Ma *(22)* for the Apollo 17 breccias). However, only a few zircons of this age have been found in the Apollo 14 rocks and no zircons of this age have been found in rocks from the Apollo 17 site. This demonstrates that the zircon ages have not been "updated" by the major 3900 Ma impacts which have reset the Ar-Ar and Rb-Sr systems. The observed zircon age distribution patterns are therefore not controlled by the late impact flux but are registering other events in the evolution of the lunar crust.

The significance of the zircon ages

Our present observations can be related to the discovery by the Lunar Prospector that the surface abundances of incompatible elements, including Th and probably other characteristic KREEP elements, are highly concentrated in a single region that encompasses Oceanus Procellarum, Mare Imbrium and the adjoining mare and highlands and is referred to as the Procellarum KREEP terrane *(23, 24)*. This concentration of Th rich material in a single region of the Moon suggests that the final portions of lunar magma ocean accumulated within this region *(e.g. 25)*, rather than being distributed as a global layer between the crust and the mantle. The Imbrium impact, represented by the Apollo 14 samples is located within the middle part of the Procellarum KREEP terrane, but the Serenitatis crater represented by Apollo 17 samples is situated at the edge of the high Th region *(26)* (Fig. 3).

The zircon age distributions suggest that the generation of KREEP magma in the region of the Apollo 17 site (Serenitatis impact crater area) ceased at about 4200 Ma, whereas it continued for another 200 to 300 Ma in the terrain that was the source of material sampled by the Apollo 14 mission (Imbrium impact crater area). Previous zircon age determinations on Apollo 17 and Apollo 14 zircons are compatible with this conclusion. Meyer et al. *(4)* reported zircon ages of granophyric clasts from Apollo 14 rocks down to ~3900 Ma. The few zircons from Apollo 17 samples previously measured all have ages in excess of 4200 Ma *(11, 20, 27)*.

Thermal modelling that assumes high heat production in this area associated with the strong enrichment of KREEP in radioactive elements suggests that a molten KREEP rich source may have existed in this region for an extended period of time *(e.g. 28)* and supported prolonged magmatic activity. If this view is correct, the lateral distribution of zircon ages may reflect shrinking of this source between 4.38 Ga and 3.90 Ga towards the middle of the Procellarum KREEP terrane. Between 4.38 and 4.20 Ga the region under the lunar crust where a molten KREEP source was present extended beyond the area highlighted by the Th anomaly and included the Apollo 17 location. However, by 4.20 Ga this region was laterally reduced to the central part of the Procellarum KREEP terrane and excluded the area of the Serenitatis impact, as indicated by the Apollo 17 zircon age record.

The dynamics of KREEP evolution

While the present data base is limited we believe that the main features of the zircon age distributions in the breccias from the Apollo 14 and 17 landing sites are sufficiently well defined to provide an insight into the dynamics of evolution of KREEP. In this we propose a history of KREEP magmatism from 4480Ma to 3900Ma

dominated by pulses of KREEPy magma generation and emplacement at 4350Ma, 4200Ma and possibly 4000Ma. This magma was generated from a deep source reservoir which itself has contracted over time.

The major peak in the zircon age distribution at ~4350 Ma represents the first generation and preservation of zircon on the Moon and the largest KREEP-magma forming event. This event was widespread as evidenced by the presence of the identical age peak in zircon age distributions for samples from Apollo 14 and Apollo 17. The significance of this event is debatable. One possibility is that it dates the formation of urKREEP as a residual accumulation of incompatible elements from the fractional crystallisation of the cooling magma ocean. However, this contradicts the W isotope data *(29, 30, 31)*, which has been interpreted as demonstrating ilmenite fractionation from the LMO about 60 Ma after the formation of the Solar system *(e.g. 32)*. These data suggest a very short period of crystallisation of the major volume of the LMO, as ilmenite is formed very late in the crystallisation sequence. Residual melt enriched in incompatible elements is left after ilmenite crystallisation and it is not clear why there is a delay of more than 100 Ma before the first zircon formed at ~4.38 Ga from this residual melt.

A second event at ~4200 Ma activated new KREEP magmatism from a now significantly contracted primary reservoir of KREEP melt. As a result of this contraction the extent of KREEP magma generation was much smaller in the area represented by the Apollo 17 samples, whereas in the area represented by Apollo 14 samples it was equal in magnitude to the 4350 Ma KREEP magma generation event. A third event at 4000 Ma resulted in a small magmatic pulse in the Imbrium impact area. The relatively small spike in the age distribution suggests that, at this time, the

region represented by the Apollo 14 site was itself on the outer margin of the continually contracting KREEP reservoir.

The above model explanation for the zircon U-Pb results introduces concepts on the timing of lunar KREEP evolution that have not been previously considered. It also forms the basis for further speculation on what was the triggering mechanism for the KREEP magma pulses.

Broadly speaking we believe there are two possible mechanisms for the triggering episodes of KREEP magmatism. The first possibility is that large impacts destabilised the primary KREEP reservoir resulting in spikes of KREEP magmatism. This mechanism would be expected to result in random pulses of KREEP magmatism possibly with a higher incidence of this magmatism early in lunar history when the impact flux was greatest. The expected smoothly declining flux is not in accord with the observed timing of KREEP age peaks. In addition there is the striking observation from the present results that essentially all the KREEPy rocks excavated by the last major impact events at ~3.9 Ga (Imbrium, Serenitatus) are significantly older than these impacts. There appears to be little KREEP magma generated by the Imbrium impact, although it is possible that KREEP rocks formed as a result of these late impacts remain deeply buried or occur elsewhere in the Procellarum KREEP Terrane.

Other explanations for the periodic production of KREEP-rich rocks, and possibly for the contraction of the primary KREEP reservoir, involve endogenic processes, and while the nature of the actual mechanisms may not be clear, they are evidently linked to the thermal history of the Moon. Recent models that attempt to explain the observed asymmetry in the concentration of Th, mare volcanism, the thickness of lunar crust etc have been summarised by Shearer et al. *(33)*. One of these models *(28)* describes the thermal evolution of the Procellarum KREEP terrane and

suggests that the accumulation of KREEP material rich in radioactive elements would result in the long term melting of the KREEP source as well as gradual heating of the underlying mantle and that Mare volcanism would span most of the Moon's history. This model does not account for the observed zircon age distribution patterns, which suggest periodic pulses of KREEP magmatic activity in the area during the first 500 Ma of lunar history. However, following this model, a possible explanation for our results envisages a build-up of radioactive heat in the KREEP reservoir until the buoyancy of the KREEP melt exceeded the strength of the overlying rocks resulting in a sudden transfer of KREEP magma and heat into the crust. The observed pattern of an initial KREEP magma pulse followed by declining magmatism could be explained by proposing that the KREEP magmatism represented the transfer of a large body of the KREEP magma from the deep reservoir to an independent, intermediate reservoir in the crust where the gradual decline in magmatism reflected the cooling of this reservoir. At the same time the deep seated reservoir gradually reheated through U, Th and K decay, until the process was repeated and a second pulse of magmatism results in the transfer of a further generation of KREEP magma into the crust. Whereas this model is consistent with our observations other possible models of the thermal history of the Procellarum KREEP Terrane could quite well fit the zircon data. However, these will need to account for the peaks in KREEP magmatic activity at ca 4350Ma, ca 4200Ma and ca 4000 Ma, the significance of the first KREEP magma pulse at 4350Ma, the paucity of ca 3850 Ma zircons (and hence KREEP rocks of this age) in the 3850±20 Ma Imbrium impact ejecta *(21)* and the lack of any zircons (KREEP rocks) younger than 4200Ma in ejecta of the 3893±9 Ma *(22)* Serenitatis event.

Conclusions

Our SIMS zircon U-Pb data confirm earlier zircon SIMS results in demonstrating that KREEP magmatism occurred on the Moon over a continuous period from 4380 to 3900Ma. However, our zircon results also demonstrate that whereas this long term igneous record is preserved in zircons from breccias from the Apollo 14 site, the record of KREEP magmatism in breccias from the Apollo 17 site extends only from 4350 to 4200Ma. In addition, our zircon SIMS measurements show that the KREEP magmatic record is irregular, consisting of two or three major magmatic episodes which are followed by declining magmatic activity. Whereas the study is constrained by the limited data set, possible complexities in the zircon U-Pb systems due to impact related resetting, and possible biasing in the sampling, we believe the data provide a close approximation to the real pattern of KREEP activity on the Moon. In explaining these observations we propose a model of KREEP magmatism involving the location of the Apollo landing sites with respect to the boundary of the lunar Th anomaly. In particular we suggest that, on the basis of the observed age distribution patterns of zircons from Apollo 14 and Apollo 17 samples, that the source reservoir for KREEP magmatism was not static but contracted from unknown initial margins towards the central part of the Procellarum KREEP terrane. Between about 4.4 and 3.9 Ga this reservoir contracted to exclude the area of Serenitatis impact, although it is possible that a much reduced molten KREEP source existed after 3.9 Ga in the centre of the terrane.

The presence of peaks and troughs in the age distribution patterns provide constraints on the mechanism responsible for the separation of magma from the KREEP reservoir and emplacement of this magma into the overlying crust. One possibility is that this separation was triggered by large meteorites that periodically

impacted the lunar surface. An alternative model is that energy, accumulated within the KREEP reservoir as a result of radioactive decay, was periodically released through magma emplacement into the overlying crust. Further research on complex zircon grains and additional analyses of zircons from breccias from other Apollo sites will be needed to resolve these issues.

Acknowledgements

In particular we would like to thank the astronauts of Apollo 14 and Apollo 17 for risking their lives to collect the samples. This study was supported by the Australian Research Council grant DP0211706 to R. Pidgeon and A. Nemchin. The NordSIM facility, (Swedish Museum of Natural History) is supported by the research councils in Denmark, Finland, Norway and Sweden together with the Swedish Museum of Natural History.

References

1. C. Meyer, R. Brett, N.J. Hubbard, D. Morrison, D. McKay, F.K. Aitken, H. Takeda, Schonfeld E., *Proc. 2nd Lunar Sci. Conf.* 393-411 (1971)
2. C. Meyer, *Phys. Chem. Earth*, **10**, 239-260 (1977)
3. B.J. Jolliff, J.M. Hughes, J.J. Freeman and R.A Zeigler, *Am. Mineral.* **91**, 1583-1595 (2006)
4. C. Meyer, I.S. Williams and W. Compston, *Meteoritics and Planetary Science*, **31**, 370-387(1996)
5. J.F. Lovering and D.A. Wark, *Proc. 2nd Lunar Sci. Conf.*, 151-158(1971)
6. C. A. Andersen,; J. R. Hinthorne, *Earth Planet. Sci. Lett.*, **14**, 195 (1972)
7. C. Meyer and V.S. Yang, *Am. Mineral.*, **73**, 1420-1425 (1988).

8. J. E. Dickinson and P. C. Hess, *Earth Planet. Sci. Lett*, **57**, 336-344 (1982)

9. P. H. Warren and J. T. Wasson, *Rev. Geophys. Space Phys.*, **17**, 73-88 (1979).

10. K. Mezger and E. J. Krogstadt, *J. Metamorphic Geol.*, **15**, 127–140 (1997)

11. W. Compston, I. S. Williams and C Meyer, *J. Geophys. Res.* **89**, 525–534 (1984)

12. R. T. Pidgeon, A. A. Nemchin, C. Meyer, *37th Annual Lunar and Planetary Science Conference, League City, Texas,* abstract no.1548 (2006)

13. C. Meyer, C. Galindo and V. Yang, *Abstracts of the Lunar and Planetary Science Conference*, **22**, 895, (1991)

14. Materials and methods are available as supporting material on *Science* Online

15. D.E. Wilhelms, *US Geological Survey Spec. Pap.* 1348 (1987)

16. L.A. Haskin, R.L. Korotev, J.J. Gillis and B.L. Jolliff, *Lunar Planet Sci. XXXIII*, 1364 (2002)

17. R.H. Morrison, V.R. Oberbeck, *Proc. Lunar Sci. Conf. 6*,2503–2530 (1975)

18. H. Hiesinger and J.W. Head, *Rev. Mineral. Geochem.*, **60**, 1-81 (2006)

19. T. Andersen, *Chem. Geol.*, **216**, 249-270 (2005)

20. R.T. Pidgeon, A.A. Nemchin, W. van Bronswijk, T. Geisler, C. Meyer, W. Compston and I. Williams, *Geochim. Cosmochim. Acta*, in press (2007)

21. D. Stöffler, G. Ryder, B.A. Ivanov, N.A. Artemieva, M.J. Cintala, and R.A.F. Grieve, *Rev. Mineral. Geochem.*, **60**: 519-596 (2006)

22. G.B. Dalrymple and G. Ryder, *J Geophys Res*, **101**, 26069-26084 (1996)

23. D.J. Lawrence, W.C. Feldman, B.L. Barraclough, A.B. Binder, R.C. Elphic, S. Maurice and D.R. Thomsen, *Science*, **281**,1484-1489 (1998)

24. D.J. Lawrence, W.C. Feldman, B.L. Barraclough, A.B. Binder, R.C. Elphic, S. Maurice, M.C. Miller and T.H. Prettyman T, *J Geophys Res*, **105**, 20307-20331 (2000)

25. M.A. Wieczorek, B.L. Jolliff, A. Khan, M.E. Pritchard, B.P. Weiss, J.G. Williams, L.L. Hood, K Righter, C.R. Neal, C.K. Shearer, I.S. McCallum, S. Tompkins, B.R. Hawke, C. Peterson, J.J. Gillis and B. Bussey, *Rev. Mineral. Geochem.*, **60**, 221-364 (2006)

26. B.L. Jolliff, J.J. Gillis, L. Haskin, R.L. Korotev and M.A. Wieczorek, *J Geophys Res*, **105**, 4197-4216 (2000)

27. C. Meyer, W. Compston and I. S. William, *Lunar and Planet. Sci. XVI*, 557-558 (1985)

28. M.A. Wieczorek and R.J. Phillips, *J Geophys Res*, **105**, 20417-20430 (2000)

29. T. Kleine, C. Münker, K. Mezger and H. Palme, *Nature*, **418**, 952-955(2002)

30. D-C Lee, A.N. Halliday, G.A. Snyder and L.A. Taylor, *Science*, **278**, 1098-1103 (1997)

31. D-C Lee, A.N. Halliday, I. Leya, R. Wieler and U. Wiechert, *Earth Planet. Sci Lett*, **198**, 267-274 (2002)

32. C.K. Shearer and H.E. Newsom, *Geochim. Cosmochim. Acta*, **64**, 3599-3613 (2000)

33. C.K. Shearer, P.C. Hess, M.A. Wieczorek, M.E. Pritchard, E.M. Parmentier, L.E. Borg, J. Longhi, L.T. Elkins-Tanton, C.R. Neal, I. Antonenko, R.M. Canup, A.N. Halliday, T.L. Grove, B.H. Hager, D-C. Lee, and U. Wiechert, *Rev. Mineral. Geochem.*, **60**, 365-518 (2006).

Figure captions

Figure 1. Concordia diagram showing all zircon analyses made during this study. Apollo 17 analyses are shown as blue ellipses and Apollo 14 analyses as red ellipses.

Figure 2. Age probability distribution plots for the Apollo 14 and Apollo 17 zircon grains superimposed on the histogram plots. Where a zircon has been subjected to multiple analysers the oldest ages accepted as the ages of the zircons.

Figure 3. Image of the near side of the Moon obtained by the Galileo mission. Apollo 14 and Apollo 17 landing sites are indicated by the white dots. The white line encloses the area of high Th concentrations (>3.5 ppm Th; Jolliff et al. 2000).

Figure 1

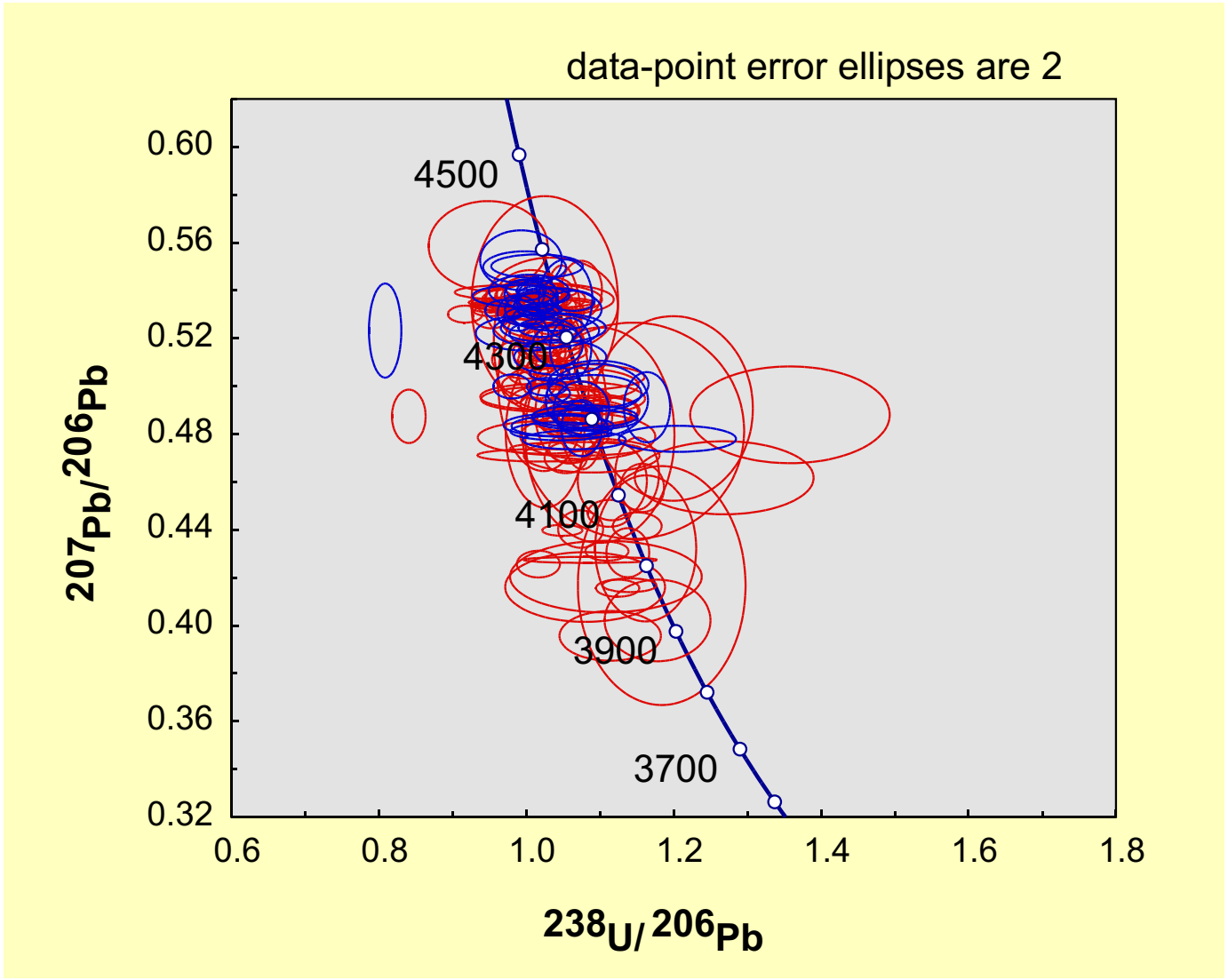
data-point error ellipses are 2
4500
4300
4100
3900
3700
0.60
0.56
0.52
0.48
0.44
0.40
0.36
0.32
0.6
0.8
1.0
1.2
1.4
1.6
1.8
207Pb/206Pb
238U/206Pb

Figure 2

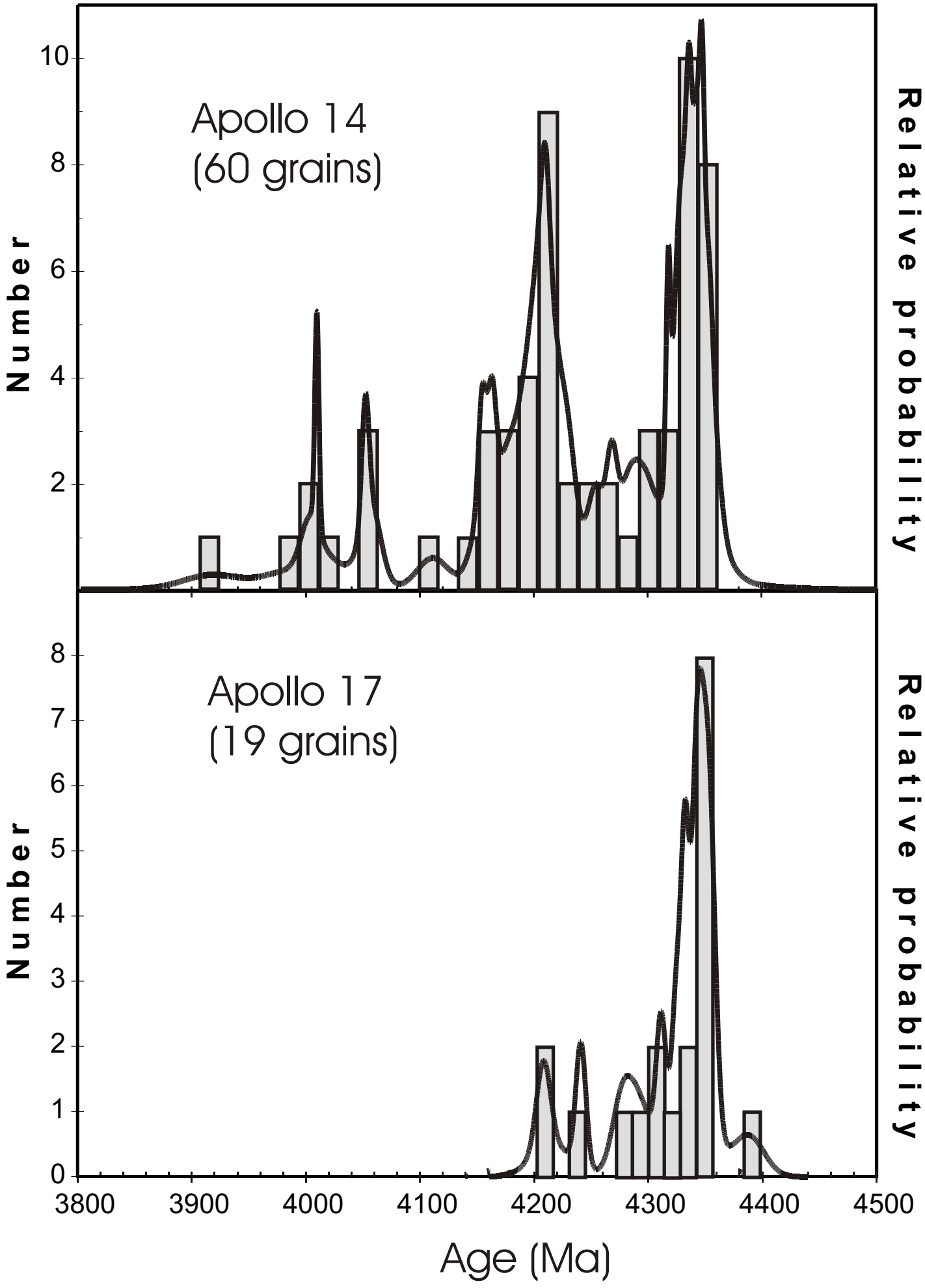
Apollo 14
(60 grains)
Apollo 17
(19 grains)
Number
Relative probability
0
1
2
3
4
5
6
7
8
10
3800
3900
4000
4100
4200
4300
4400
4500
Age (Ma)

Figure 3

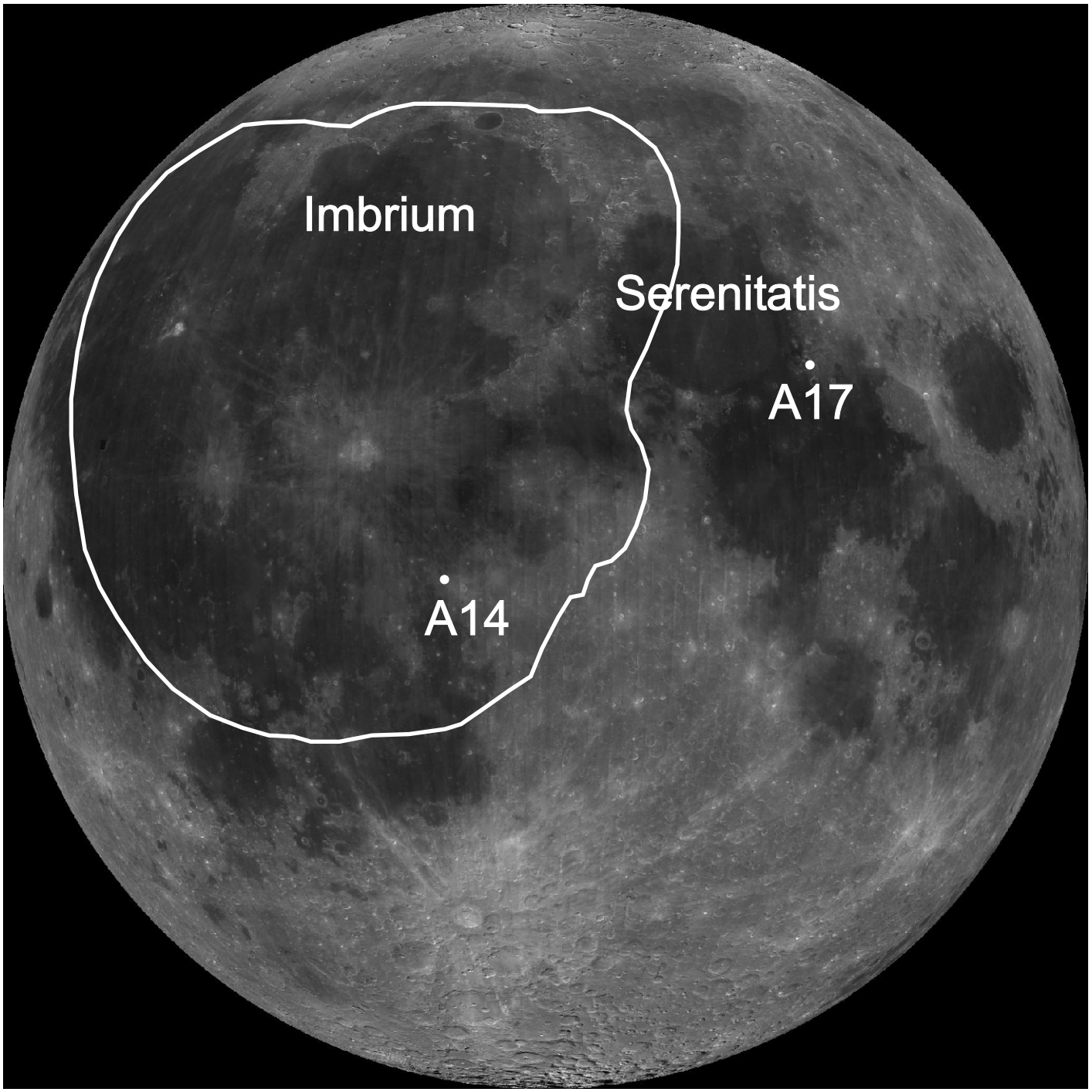

Supporting Online Material

Materials and methods

Ten sections analysed using ims1270 instrument in Stockholm and six analysed using SHRIMPII ion probe in Perth are listed in the table S2. All errors for the data obtained in this work are 2-sigma.

IMS 1270 analytical conditions

The SIMS methodology used at the Nordsim facility closely follows previously published analytical descriptions *(S1, S2)*. A molecular oxygen beam (O_2^-) at -13 kV was imaged through an aperture, giving a ca. 6 nA current in an elliptical, ca. 20 μm spot. Secondary ions were extracted from the sample at +10 kV and admitted, via high magnification transfer optics, to the mass spectrometer operating at a mass resolution (M/ΔM) of 5300. Oxygen flooding of the sample chamber was used to enhance Pb^+ yield. At the start of each analysis, a 2 minute pre-sputter raster over 25 μm was used to remove the Au coating to minimise surface contamination. This was followed by automated centring of the beam in the field aperture, optimisation of mass calibration using selected high-intensity peaks of the mono-collection routine and optimisation of secondary ion energy in the 60 eV energy window. The peak-hopping data collection routine consisted of 16 cycles through the mass stations, with signals measured on an ion counting electron multiplier with a 44 ns electronically gated dead time. Pb/U ratios were calibrated using an empirical correlation between Pb^+/U^+ and UO_2^+/U^+ ratios, normalised to the 1065 Ma Geostandards 91500 zircon *(S3)*. For zircon grains located in thin sections, standard measurements from 91500 mounted in a polished epoxy mount were used; test with another epoxy mount

showed that there was no significant (> ca. 1.2%) bias on Pb/U ratios as a result of the off mount calibration procedure.

SHRIMPII analytical conditions

The SHRIMP methodology follows analytical procedure described by Compston et al. *(S4)* and Kennedy and de Laeter *(S5)*. The filtered (O_2^-) beam with intensity between 3 and 4 nA was focused on the surface of samples into ca 20 μm spot. Secondary ions were passed to the mass spectrometer operating at a mass resolution (M/ΔM) of ~5000. Each analysis was preceded by a 3 minute rastering to remove the Au coating. The peak-hopping data collection routine consisted of 7 scans through the mass stations, with signals measured on an ion counting electron multiplier. Pb/U ratios were calibrated using an empirical correlation between Pb^+/U^+ and UO^+/U^+ ratios, normalised to the 564 Ma Sri-Lankan zircon CZ3 *(S6)*. The 1.5 to 1.8% error obtained from the multiple analyses of Pb/U ratio in the standard during individual SHRIMP sessions was added in quadrature to the errors observed in the unknowns. The initial data reduction was done using SQUID AddIn for Microsoft Excel *(S7)* and Isoplot *(S8)* was applied for further age calculations.

Initial Pb correction

Initial Pb correction of lunar samples is complicated by the very radiogenic Pb compositions of many lunar rocks *(e.g. S9, S10)* which suggest a substantial loss of Pb from the Moon. Meyer et al. *(S11)* applied a complicated procedure to correct their zircon analyses for the initial Pb composition. This procedure assumed that the initial Pb is a mixture of Canyon Diabolo troilite Pb and some radiogenic component. The

mixing equations were solved by considering Th-Pb and U-Pb systems simultaneously.

Most of zircon analyses in the present study have extremely low proportions of ^{204}Pb, suggesting a very small contribution of initial Pb. This results in almost identical values for initial Pb-corrected and uncorrected ratios in most analysed grains. Consequently the results are not sensitive to the choice of the composition for the initial Pb. In addition, proportion of ^{204}Pb appears to be consistently high in zircons from some thin sections, but not others even when they represent the same samples. For example overall proportion of ^{204}Pb in the section 14303-52 appears to be significantly higher than in the section 14303-49 (Table S1). This suggests that most of non-radiogenic Pb in the analysed zircons is the surface contamination. With this assumption all zircon analyses were corrected using Stacey-Kramers *(S12)* model, modern, common Pb compositions.

References

S1. M. J. Whitehouse, B. S. Kamber and S. Moorbath, *Chem. Geol.*, **160**, 201-224, (1999)

S2. Whitehouse and Kamber, *J. Petrol.*, **46**, 291-318 (2005)

S3. M. Wiedenbeck, J. Hanchar, W.H Peck, P. Sylvester, J. Valley, M. Whitehouse, A Kronz,. Y. Morishita, L. Nasdala, & twenty one others. G*eostandards and Geoanalytical Research,* **28,** 9-39, (2004).

S4. W. Compston, I. S. Williams and C Meyer, *J. Geophys. Res.* **89**, 525–534 (1984)

S5. A.K. Kennedy and J.R.de Laeter, *In: 8th Int. Conf. on on Geochronology, Cosmochronology and Isotope Geology*, Berkeley, U.S. Geol. Surv. Circ. 1107, p.166 (1994).

S6. R.T. Pidgeon, D. Furfaro, A.K. Kennedy, A.A. Nemchin, and W. van Bronswjk, *In: 8th Int. Conf. on Geochronology, Cosmochronology and Isotope Geology*, Berkeley, U.S. Geol. Surv. Circ. 1107, p. 251 (1994).

S7. K. Ludwig, "Users manual for Squid1.02" (Berkeley Geochronology Center, Special Publication 1a, 19pp, 2001)

S8. K. Ludwig, "Users manual for Isoplot/Ex rev. 2.49" (Berkeley Geochronology Center, Special Publication *2,* 55pp. 2001)

S9. F. Tera and G. J. Wasserburg, *Earth Plane. Sci. Lett,* **14**, 281-304 (1972)

S10. N. H. Gale, *Earth Plane. Sci. Lett,* **17**, 65-78 (1972)

S11. C. Meyer, I.S. Williams and W. Compston, *Meteoritics and Planetary Science*, **31**, 370-387(1996)

S12. J.S. Stacey and J.D. Kramers, *Earth Plane. Sci. Lett,* **26**, 207-221 (1975)

Table S1 U-Pb ages of analysed zircons from Apollo 14 and Apollo 17 missions

Sample and analysis	U (ppm)	Th (ppm)	Th/U	f206%	% disc	$\frac{^{207}Pb}{^{206}Pb}Age(Ma)$	Grain location
Apollo 14 samples							
Crystalline matrix breccia (Simonds et al, 1977); analysed using SHRIMP							
14066-47-1-1*	25	11	0.45	3.82	-5	4177±17	breccia matrix
14066-47-2-1	123	62	0.53	0.18	-4	4352±7	breccia matrix
14066-47-3-1	39	13	0.34	0.95	-1	4226±17	breccia matrix
14066-47-4-1	126	50	0.41	0.34	-2	4162±7	breccia matrix
14066-47-5-1	271	152	0.58	0.89	-6	4153±7	breccia matrix
Light matrix breccia (Simonds et al, 1977); analysed using IMS1270							
14083-35-1-1	57	35	0.87	0.28	-7	4325±12	breccia matrix
14083-35-2-1	225	260	1.32	0.08	-7	4051±6	breccia matrix
14083-35-3-1	30	15	0.49	0.19	1	4057±16	breccia matrix
14083-35-4-1	75	36	0.51	0.16	-3	4163±16	breccia matrix
14083-35-5-1	28	24	1.63	1.65	-20	4204±28	breccia matrix
14083-35-6-1	207	79	0.38	0.02	-3	4263±13	breccia matrix
14083-35-6-2	241	98	0.41	0.01	-4	4267±9	
14083-35-7-1	101	62	0.60	0.02	-2	4209±9	breccia matrix
14083-35-7-2	43	14	0.33	0.12	-2	4215±13	
Crystalline matrix breccia (Simonds et al, 1977); analysed using IMS1270 All zircon grains are from the same clast containing melt and Pl crystals							
14303-49-1-1	74	27	0.37	2.58	-3	4338±9	
14303-49-1-2	74	24	0.34	0.16	-2	4298±9	
14303-49-2-1	149	64	0.48	2.17	-2	4296±15	
14303-49-2-2	199	135	0.81	2.53	-4	4327±10	

Table 1 (continued)

Sample and analysis	U (ppm)	Th (ppm)	Th/U	f206%	% disc	$\frac{^{207}Pb}{^{206}Pb}Age(Ma)$	Grain location
14303-49-3-1	541	319	0.60	0.12	-1	4316±4	
14303-49-4-1	574	350	0.67	0.15	-2	4346±4	
Crystalline matrix breccia (Simonds et al, 1977); analysed using IMS1270							
14303-52-1-1	41	27	0.76	0.55	-10	4002±16	breccia matrix
14303-52-2-1	305	418	1.49	0.46	-7	4335±5	breccia matrix
14303-52-3-1	67	50	0.73	23.02	0	4179±111	norite clast
14303-52-3-2	62	47	0.79	0.33	0	4313±58	
14303-52-3-3	61	29	0.50	9.10	2	4129±39	
14303-52-4-1	46	26	0.48	42.55	-1	4340±98	breccia matrix
14303-52-5-1	164	111	0.69	0.44	-1	4209±7	breccia matrix
14303-52-5-2	134	93	0.71	6.14	-3	4205±19	
14303-52-6-1	47	23	0.47	1.03	-1	4306±13	breccia matrix
14303-52-6-2	68	33	0.49	0.81	-3	4328±12	
14303-52-6-3	76	41	0.54	1.03	-1	4343±10	
14303-52-7-1	44	24	0.55	0.34	-1	4320±13	breccia matrix
14303-52-8-1	88	59	0.72	6.39	-4	4150±16	breccia matrix
14303-52-9-1	76	54	0.68	8.38	2	4110±27	breccia matrix
14303-52-10-1	69	28	0.43	40.17	-5	4295±59	breccia matrix
14303-52-11-1	61	16	0.20	15.47	-2	4207±51	breccia matrix
Crystalline matrix breccia of Fra Mauro type (Simonds et al, 1977); analysed using IMS1270							
14305-19-1-1	1457	1639	1.23	2.95	-10	4327±8	breccia matrix
14305-19-2-1	107	87	0.93	13.51	-3	4264±30	breccia matrix
14305-19-3-1	60	36	0.51	25.26	3	4355±26	breccia matrix
14305-19-4-1	43	22	0.39	22.62	1	3970±143	breccia matrix

Table 1 (continued)

Sample and analysis	U (ppm)	Th (ppm)	Th/U	f206%	% disc	$\frac{^{207}Pb}{^{206}Pb}Age(Ma)$	Grain location
14305-19-4-2	124	76	0.62	2.36	-1	4019±29	
14305-19-5-1	36	12	0.35	1.01	-3	4282±16	breccia matrix
14305-19-6-1	51	16	0.12	44.50	0	4216±63	attached to Pl grain
14305-19-6-2	88	28	0.31	1.64	-2	4298±26	
Crystalline matrix breccia (Simonds et al, 1977); analysed using SHRIMP							
14306-150-1-1	73	42	0.60	0.09	1	4345±10	breccia matrix
14306-150-1-2	76	43	0.61	0.07	0	4345±9	
14306-150-2-1	83	45	0.57	0.34	-3	4338±10	breccia matrix
14306-150-2-2	41	13	0.35	1.17	0	4330±12	
14306-150-3-1	154	85	0.61	0.05	-7	4333±6	breccia matrix
14306-150-4-1	151	57	0.39	0.07	-1	4075±15	fragments of grain in norite clast
14306-150-4-2	154	49	0.35	0.14	-3	3967±10	
14306-150-4-3	121	70	0.60	0.18	-2	3971±8	
14306-150-4-4	78	60	0.77	0.20	-2	4184±19	
14306-150-4-5	137	82	0.71	0.48	-5	4183±78	
Crystalline matrix breccia (Simonds et al, 1977); analysed using SHRIMP All grains are from the same norite clast							
14306-60-1	39	22	0.59	2.07	-2	4192±12	
14306-60-2	26	16	0.63	0.93	1	4211±14	
14306-60-3	44	30	0.71	0.95	1	4205±12	
14306-60-4	29	17	0.62	7.16	-2	4202±23	
14306-60-5	11	4	0.36	24.85	3	4185±113	
14306-60-6	33	16	0.49	0.28	-3	4200±12	
14306-60-7	33	20	0.61	1.69	1	4205±15	

Table 1 (continued)

Sample and analysis	U (ppm)	Th (ppm)	Th/U	f206%	% disc	$\frac{^{207}Pb}{^{206}Pb}Age(Ma)$	Grain location
Crystalline matrix breccia (Simonds et al, 1977); analysed using IMS1270							
14321-16-1-1	87	48	0.65	14.78	-5	4053±21	anorthosite clast
14321-16-1-2	79	41	0.29	39.33	1	4025±85	
14321-16-1-3	130	45	0.38	1.04	-3	4021±11	
Crystalline matrix breccia (Simonds et al, 1977); analysed using SHRIMP							
All grains are from the sawdust							
14321-2-1	8	3	0.37	0.29	-4	3984±44	
14321-2-2	7	3	0.37	0.77	-6	3968±43	
14321-1-1	808	333	0.43	0.03	-5	4008±4	
14321-20-1	30	10	0.35	0.30	-1	4344±15	
14321-20-2	32	12	0.38	0.47	-2	4344±15	
14321-20-1	33	11	0.35	0.05	-2	4316±13	
14321-20-2	33	12	0.37	0.02	-3	4346±13	
14321-12-1	225	104	0.48	0.10	-2	4338±6	
14321-12-2	263	127	0.50	0.11	-2	4341±5	
14321-11-1	52	28	0.55	0.30	0	4252±13	
14321-11-2	31	18	0.61	0.46	-1	4243±17	
14321-10-1	51	29	0.59	0.48	-4	4228±13	
14321-10-2	53	29	0.56	0.54	-4	4225±13	
14321-8-1	15	6	0.43	1.05	15	4205±50	
14321-8-2	16	5	0.33	1.41	9	4123±40	
14321-13-1	61	26	0.44	0.22	-5	4404±40	
14321-13-2	64	30	0.47	0.14	-1	4338±45	
14321-14-1	88	31	0.37	0.16	-1	4178±24	
14321-14-2	82	29	0.36	0.29	-1	4153±18	

Table 1 (continued)

Sample and analysis	U (ppm)	Th (ppm)	Th/U	f206%	% disc	$\frac{^{207}Pb}{^{206}Pb}Age(Ma)$	Grain location
14321-14-3	89	33	0.39	0.05	0	4119±43	
14321-21-1	50	26	0.54	0.03	-2	4284±11	
14321-21-2	51	27	0.55	0.01	-5	4274±19	
14321-21-3	78	43	0.57	0.03	-2	4295±18	
14321-24-1	12	4	0.34	0.62	-6	3893±32	
14321-24-2	13	4	0.34	0.15	-1	3917±52	
14321-100-1	80	49	0.64	0.02	-1	4336±15	
14321-100-2	83	53	0.66	0.07	-3	4336±12	
14321-100-3	42	22	0.54	0.05	-2	4348±14	
14321-25-1	19	6	0.35	0.05	-4	4245±89	
14321-25-2	19	7	0.40	0.07	7	4213±95	
14321-22-1	60	38	0.66	0.10	-2	4349±23	
14321-22-2	55	35	0.66	0.12	-1	4358±11	
14321-23-1	23	8	0.38	0.03	-2	4218±21	
14321-23-2	38	20	0.54	0.04	1	4211±16	
Apollo 17 samples							
Aphanitic impact melt breccia (James et al, 1976); analysed using IMS1270							
73215-122-1-1	65	27	0.43	0.20	-3	4349±14	inside a small Pl grain
73215-122-1-2	68	28	0.44	0.05	-2	4324±10	
73215-122-1-3	71	27	0.40	0.30	-4	4328±17	
73215-122-2-1	199	79	0.41	0.06	-3	4240±9	breccia matrix
73215-122-2-2	213	88	0.43	0.20	-3	4232±10	
73215-122-3-1	69	25	0.36	0.01	-1	4189±29	breccia matrix

Table 1 (continued)

Sample and analysis	U (ppm)	Th (ppm)	Th/U	f206%	% disc	$\frac{^{207}Pb}{^{206}Pb}Age(Ma)$	Grain location
73215-122-3-2	53	17	0.31	0.03	5	4215±36	
Aphanitic impact melt breccia (James et al, 1976); analysed using IMS1270							
72215-195-1-1	81	45	0.57	0.24	-2	4380±14	breccia matrix
72215-195-1-2	88	49	0.57	0.16	-2	4388±27	
72215-195-1-3	32	10	0.34	0.48	0	4333±20	
72215-195-1-4	153	96	0.65	0.08	-2	4354±15	
72215-195-1-5	108	62	0.59	0.09	-1	4381±11	
Impact melt breccia (Ryder, 1993); analysed using IMS1270							
73217-52-1-1	252	216	1.00	0.06	-7	4241±12	edge of the mount; matrix
73217-52-1-2	185	116	0.93	0.42	-20	4308±45	
73217-52-2-1	166	82	0.50	0.04	-2	4332±6	breccia matrix
73217-52-2-2	169	90	0.55	0.02	-2	4331±7	
Aphanitic impact melt breccia (Ryder, 1993); analysed using IMS1270							
73235-54-1-1	36	12	0.34	0.32	-1	4290±20	breccia matrix
73235-54-2-1	91	26	0.31	0.07	-3	4324±8	breccia matrix
73235-54-3-1	63	36	0.59	0.09	-2	4344±13	breccia matrix
73235-54-3-2	64	37	0.60	0.06	-3	4355±10	
73235-54-4-1	69	27	0.43	0.29	-5	4332±10	breccia matrix
73235-54-4-2	41	14	0.40	0.13	0	4287±30	
Aphanitic impact melt breccia (Ryder, 1993); analysed using IMS1270							
73235-80-1-1	10	5	0.52	0.72	-1	4213±28	breccia matrix
73235-80-1-2	10	5	0.51	0.32	1	4345±37	

Table 1 (continued)

Sample and analysis	U (ppm)	Th (ppm)	Th/U	f206%	% disc	$\frac{^{207}Pb}{^{206}Pb}Age(Ma)$	Grain location
73235-80-2-1	98	57	0.59	0.05	-2	4338±10	breccia matrix
73235-80-2-2	94	56	0.61	0.03	-2	4342±8	
Aphanitic impact melt breccia (Ryder, 1993); analysed using IMS1270							
73235-60-1-1	173	92	0.52	0.01	2	4342±9	breccia matrix
73235-60-2-1	140	77	0.54	0.03	-4	4305±10	breccia matrix
73235-60-2-2	124	65	0.49	0.03	-2	4347±16	
73235-60-3-1	85	28	0.32	0.07	-1	4201±11	attached to Pl grain
73235-60-3-2	82	29	0.34	0.03	-1	4207±12	
73235-60-4-1	107	67	0.60	0.03	-2	4353±11	breccia matrix
Aphanitic impact melt breccia (Ryder, 1993); analysed using SHRIMP							
73235-82-1-1	106	52	0.51	0.16	-3	4348±10	multiple fragments in anorthosite clast
73235-82-1-2	52	27	0.53	0.02	-2	4308±17	
73235-82-1-3	65	29	0.45	0.05	-4	4305±17	
73235-82-1-4	62	32	0.52	0.10	-1	4311±14	
Impact melt breccia (Simonds et al, 1975); analysed using SHRIMP							
76295-91-1-1	129	69	0.52	0.04	1	4257±7	breccia matrix
76295-91-1-2	88	46	0.51	0.06	0	4311±8	
76295-91-2-1	54	30	0.58	0.29	-1	4276±17	breccia matrix
76295-91-2-2	40	23	0.59	0.02	2	4243±24	
76295-91-2-3	60	39	0.66	0.11	1	4233±18	
76295-91-2-4	40	23	0.59	0.12	1	4224±37	
76295-91-2-5	55	35	0.65	0.21	5	4226±51	

*Sample-Section-Grain-Spot